Macromolecules
ARTICLE

Macromolecules **2010**, *43*, 8115–8120 **8115**
DOI: 10.1021/ma1015903

Low Band Gap Polymers for Roll-to-Roll Coated Polymer Solar Cells

Eva Bundgaard,* Ole Hagemann, Matthieu Manceau, Mikkel Jørgensen, and Frederik C. Krebs

Risø DTU National Laboratory for Sustainable Energy, Technical University of Denmark, Frederiksborgvej 399, DK-4000 Roskilde, Denmark

Received July 15, 2010; Revised Manuscript Received August 26, 2010

ABSTRACT: We present the synthesis of a low band gap copolymer based on dithienothiophene and dialkoxybenzothiadiazole (poly(dithienothiophene-*co*-dialkoxybenzothiadiazole), PDTTDABT). The optical properties of the polymer showed a band gap of 1.6 eV and a sky-blue color in solid films. The polymer was explored in roll-to-roll coating experiments and was optimized with respect to the manufacturing process and mixing ratio with [60]PCBM through a series of experiments with variation of the composition in steps of 1% w/w of respectively PDTTDABT and [60]PCBM and a relatively broad optimimum was found around a 1:2 mixing ratio. Roll-to-roll coated polymer solar cell devices were prepared under ambient conditions employing solution processing in all steps including the metallic back electrode that was printed as a grid giving semitransparent solar cell devices. Solar cell modules comprising 16 serially connected cells were prepared with a total module active area of 96 cm^2. The devices were tested for operational stability under simulated sunlight (AM1.5G) and natural sunlight, and the photochemical stability of the polymer was examined using a combination of UV−vis and IR spectroscopy.

Introduction

Research on organic photovoltaics (OPV) has in the past decade intensified significantly with a resulting increase in both the efficiency and stability. Polymer and organic solar cells are now viewed by many as being on their way to become a true competitor to the thin film inorganic photovoltaics. Critics have voiced opinions against this view based on thorough examination of the business and market possibilities with the technology at hand, and the actual performance reached with the technology currently and with the projected marvels of the technology.[1] The field of OPV has been reviewed numerous times in recent years,[2] and most recently power conversion efficiencies above 8% have been claimed[3] and OPV has been demonstrated publically in several very convincing cases.[4] One of the most important problems to address if the field of OPV is to convincingly waive off the strong criticism is that the challenge to unite efficiency, stability, and production in a single material is efficiently met.[5] This naturally assumes that the material at hand has good power conversion efficiency, good photochemical stability and a good stability during operation in a solar cell device. The materials must however also enable efficient large scale manufacture in an industrially relevant setting.[6] This implies that the synthetic route has to be simple and the physical behavior in solution during coating and drying to a solid film is compatible with the manufacturing approach. This may seem trivial at first but actually presents a significant challenge, and it is likely that many of the reported highly performing polymers are not compatible with some of the large area roll-to-roll (R2R) processes that have been developed or they are not photochemically stable to meaningfully enable reliable operation in a practical setting removed from the often idealized laboratory glovebox setting that polymer solar cells are normally studied under. In the standard laboratory setting, the active layer of the solar cell is spin-coated from an organic solvent at ambient temperature followed by completion of the device by evaporation of a metal electrode. The device film does thus not experience high temperatures during the manufacture. Even if the morphology of the active layer is not thermally stable, this approach quite readily enables the preparation of efficient devices that can be characterized. If, however, the manufacturing process required extra heating steps, the final device would never exhibit any significant performance. We have found that it is actually rare that conjugated polymer materials provide thermally stable morphologies in bulk heterojunction mixtures with fullerenes such as [6,6]-phenyl-C_{61}-butyric acid methyl ester ([60]PCBM). The classical polymer of OPV is poly(3-hexylthiophene) (P3HT) that gives uniquely stable nanomorphologies when mixed with [60]PCBM that are thermally stable at high temperatures (150−180 °C) for extended periods of time. This has enabled the use of P3HT:[60]PCBM mixtures in industrially roll-to-roll processed polymer solar cells where all layers are processed by solution methods. One of the well-developed and well-described processes known as ProcessOne[6] presents an inverted geometry where a flexible carrier substrate such as polyethyleneterphthalate (PET) is uniformly coated with indium−tin−oxide (ITO) that is then patterned into stripes followed by deposition of an electron transport layer (ETL) in the form of soluble zinc oxide nanoparticles that can be coated from solution. The deposition of the active layer on top employs drying of the active layer at a temperature of 140 °C for 30−60 s. In principle, the drying could be done at lower temperature or room temperature by spending more time in the drier (longer drier or lower speed). The processing of the subsequent layers; the hole transport layer (HTL) which typically is in the form of poly(3,4-ethylenedioxythiophene):poly(styrenesulfonate) (PEDOT:PSS) and the printable metallic back electrode does require drying at temperatures of 140 °C for periods of time in the range of 5−10 min and unless the active layer presents a thermally stable nanomorphology it will not be compatible with such a process. It is thus of some significance to develop low band gap polymer materials that can be coated or printed and present a

*Corresponding author. E-mail: evbu@risoe.dtu.dk.

Published on Web 09/15/2010

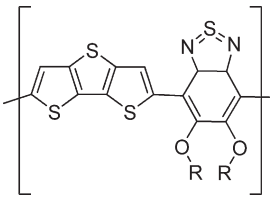

Figure 1. Poly(dithienothiophene-*co*-dialkoxybenzothiadiazole), PDTTDABT. R = $C_{14}H_{27}$.

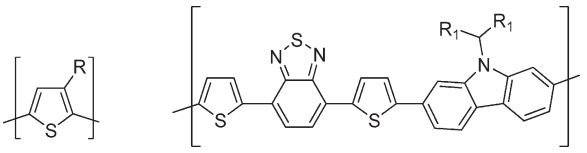

Figure 2. Reference polymers used in this work: (left) poly-(3-hexylthiophene), P3HT; (right) poly(*N*-9″-heptadecanyl-2,7-carbazole-*alt*-5,5-(4′,7′-di-2-thienyl-2′,1′,3′-benzothiadiazole)), PCbzTBT. R = C_6H_{13}; R_1 = C_8H_{17}.

thermally stable nanomorphology that enable heating for extended periods of time during drying of subsequently processed layers and electrodes.

In this paper, we present the synthesis of low band gap polymer, PDTTDABT (Figure 1), and fully characterize it with respect to the fundamental properties and behavior in small model solar cells. We further describe the use of the material in the manufacture of polymer solar cells by R2R slot-die coating and demonstrate that it has a nanomorphology with a reasonable thermal stability and a reasonable photochemical stability. We compare this to a recently described high performance polymer that did not enable R2R processing using ProcessOne nor showed a significant photochemical stability (Figure 2).

Experimental Section

Synthesis. Dithieno[3,2-*b*:2′,3′-*d*]-thiophene[7] and 4,7-dibromo-5,6-bis(tetradecyloxy)benzo[c][1,2,5]thiadiazole[8] were prepared as described in the literature.

Tributyltin Dithieno[3,2-*b*:2′,3′-*d*]-thiophene. Dithieno[3,2-*b*:2′,3′-*d*]-thiophene (0.98 g, 50 mmol) was dissolved in dry THF (30 mL) and cooled to −78 °C. *n*BuLi (7.2 mL+ 0.8 mL, 2.3 equiv of 1.6 M) was added dropwise. When the reaction was completed (^{1}H NMR test) tributyltin chloride (4.86 g, 150 mmol) was added and the reaction mixture was allowed to reach room temperature. The reaction mixture was evaporated and purified by column chromatography on basic aluminum oxide using 5% Et_3N in hexane as eluent to give the product in 53% yield (2.0 g).

^{1}H NMR (500 MHz) δ: 7.26 (s, 2H), 1.65−1.57 (m, 12H), 1.38 (m, 12H), 1.16 (t, 12H, J = 8 Hz), 0.93 (t, 18H, J = 7 Hz).

^{13}C NMR (75 MHz) δ: 143.6, 138.7, 136.1, 128.0, 28.9, 27.3, 13.6, 11.0.

Poly(dithienothiophene-*co*-dialkoxybenzothiadiazole), PDTTDABT. Tributyltin dithieno[3,2-*b*:2′,3′-*d*]-thiophene (278 mg, 0.36 mmol) and 4,7-dibromo-5,6-bis(tetradecyloxy)benzo[c]-[1,2,5]thiadiazole (225 mg, 0.31 mmol), $Pd_2(dba)_3$ (20 mg, 7 mol %), and tri(*O*-tolyl)phosphine (54 mg, 56 mol %) were dissolved in dry toluene (30 mg/mL) and degassed with argon. The reaction was refluxed for 24 h and the resulting polymer was precipitated in MeOH (120 mL). Purification was done by Soxhlet extraction using methanol, heptane, and chloroform as solvents. The polymer was precipitated from the chloroform fraction with methanol (120 mL). Yield = 75% (analytical data is given in the Supporting Information).

Solar Cells. The polymer (PDTTDABT or PCbzTBT) and the chosen fullerene were dissolved in chlorobenzene (concentration 20 mg/mL) and stirred at 30 °C for 2 h. The active area of the small area cells were 0.5 cm^2 and 96 cm^2 for the R2R coated modules. Geometry of the devices were normal: ITO/PEDOT:PSS/active layer/Al inverted: ITO/ZnO/active layer/PEDOT:PSS/Ag.

Small Area Cells with Evaporated Electrodes: Normal Devices. ITO-coated glass slides were spin coated with PEDOT:PSS (from Aldrich, filtered through 1 μm filter, 2800 rpm) followed by spin coating of the active layer (filtered through 1 μm filter, 1000 rpm). The devices were finished with evaporation of the Al electrode in a vacuum chamber (10^{-7} mBar).

Small Area Cells with Evaporated Electrodes: Inverted Devices. ITO-coated glass slides were spin coated with ZnO (45 mg/mL ZnO nanoparticles in acetone/methanol solution, 1000 rpm), followed by spin coating of the active layer (filtered through 1 μm filter, 1000 rpm) and PEDOT:PSS (5010 from AGFA diluted with isopropanol to a viscosity of 270 mPa·s, 1000 rpm). The devices were finished by evaporation of the Ag electrode in a vacuum chamber (10^{-7} mBar).

Roll-to-Roll Processed Modules with Printed Electrode. The polymer (PDTTDABT or PCbzTBT) (200 mg, 1:1) and [60]PCBM (200 mg) were dissolved in chlorobenzene/$CHCl_3$ (1:1, 8 mL) and stirred at 30 °C for 2 h. The modules were prepared as described in the literature.[6]

Indoor Testing. The small area devices were characterized under a solar simulator (AM 1.5, 1000 W m^{-2}, 55 ± 5 °C using a wing fan) using a Keithley 2400 sourcemeter. The R2R coated large area modules were characterized R2R under a solar simulator (AM 1.5, 1000 W m^{-2}) and then cut into individual modules and characterized again under a solar simulator (AM 1.5, 1000 W m^{-2}).

Outdoor Testing. Modules were tested outdoors in Denmark on the 14th of October, 2009, at midday (AM1.5G, WGS84: 55°69′N/12°10′E). The temperature was 19 °C and the illumination was measured with a pyranometer to 998 W m^{-2}.

Photochemical Stability. Pure polymer samples (PDTTDABT, P3HT, and PCbzTBT) were spin-coated at 1500 rpm on KBr plates from chlorobenzene solutions (25, 20, and 17 g L^{-1} respectively). Solution concentrations were adapted to get a maximum peak absorbance of about 0.8 for each material. The films were illuminated under solar simulation (AM1.5G, 1000 W m^{-2}, 85 °C). The films were removed periodically and UV−vis and IR spectra were recorded to monitor the degradation. UV−visible absorbance spectra were recorded between 200 and 1100 nm. IR spectra were recorded in transmission mode (4 cm^{-1} resolution, 32 scans summation).

Results and Discussion

Synthesis. Higher power conversion efficiency is achievable when a low band gap polymer is used in the OPV device.[9−12] A low band gap polymer has a band gap below 2 eV. The low band gap of the polymer can be achieved in different ways; one way is to use a donor−acceptor system. Several examples of low band gap polymers in the literature are based on this type of system.[9−13] The donor is often thiophene, carbazole, or cyclopentadithiophene and many different heterocycles such as benzothiadiazole and thienopyrazine have been applied as acceptor units. The choice of donor and acceptor is crucial to achieve the optimum band gap which is believed to be around 1.7−1.4 eV.

PDTTDABT is based on a donor−acceptor system, dithienothiophene and benzothiadiazole, respectively. The dithienothiophene unit was chosen as donor unit instead of thiophene due to the flat structure of the fused ring system, thus being able to increase the conjugation length of the polymer and thus decreasing the band gap.

The ditributyltin dithiophene is prepared from dithienothiophene by lithiation with *n*BuLi and reaction with tributyltinchloride. The donor is coupled with the dibromo

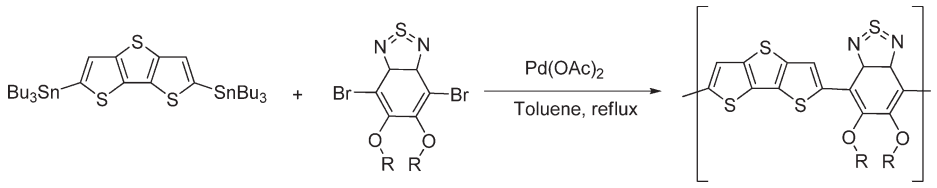

Figure 3. Synthesis of PDTTDABT. R = $C_{14}H_{27}$.

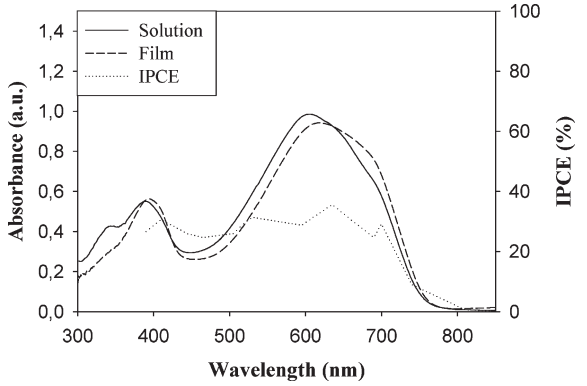

Figure 4. UV−vis ($CHCl_3$ solution and film spin coated from $CHCl_3$, 20 mg/mL) and IPCE for PDTTDABT (small area solar cells).

derivate of the acceptor in a Stille cross coupling reaction overnight resulting in a blue polymer solution (Figure 3). The polymerization proceeded quite efficiently and was carried out a number of times to optimize the synthesis. The polymer material was purified by Soxhlet extraction with acetone and methanol and was finally liberated with chloroform. High molecular weight products could be obtained and a bimodal molecular weight distribution was observed for most of the batches (see Supporting Information). We ascribe this observation to unwanted termination reactions during the polymerization. The molecular weight of the first batch was very low, which is ascribed to the use of trimethyltin-dithienothiophene instead of the tributyltin derivative; thus, the low molecular weight resulting from the faster degradation of the trimethyltin derivate during the reaction is observed.

Optical Properties. In Figure 4 the UV−vis spectrum of PDTTDABT in solution and as a film is shown along with the IPCE curve. PDTTDABT is deep blue in solution and gives sky blue solid films that absorb light with wavelengths up to around 780 nm corresponding to a band gap of 1.6 eV. A small red shift is seen for the polymer film as compare to solution. The IPCE has a broad peak around 38% from 500 to 700 nm symbatic with the absorption curve. For comparison the IPCE for PCbzTBT/$PC_{70}BM$ devices with a TiO_x optical spacer layer was 70% from 400 to 600 nm on optimized devices.[14]

Device Performance. *Small Area Devices with Evaporated Electrodes* (*Normal and Inverted*). PDTTDABT was studied in small area solar cells (0.5 cm^2) before preparing the large modules described below. The highest performance measured was I_{SC} of −7.99 mA cm^{-2}, V_{OC} of 0.49 V, fill factor of 28%, and η of 2.2% for a device based on the batch for the optimized synthesis in a 1:1 mixture with [60]PCBM and annealed for 5 min at 130 °C (see Supporting Information for photovoltaic performances for devices based on the different batches and IV curves). OPV devices based on the first batch were not prepared due to the low molecular weight (M_w = 2600 g/mol).

The photovoltaic performance of the solar cells showed that annealing of the device generally improved the efficiency. The use of either $PC_{70}BM$ or *bis*-PCBM did not result in improved efficiencies mainly due to the lower V_{OC} which is obtained when the energy difference between the highest occupied molecular orbital (HOMO) of the donor and the lowest unoccupied molecular orbital (LUMO) of the acceptor is lowered.[9,11,15] For the small area devices the highest performances were obtained for inverted devices with a ratio between polymer and fullerene of 1:1. In comparison devices with normal and inverted device structure based on reference polymers, PCbzTBT and P3HT, showed the highest efficiencies for devices with a normal geometry. This is noteworthy since the device structure applied in ProcessOne is the inverted structure.[6] The reference polymers has reported efficiencies of 6.1% for PCbzTBT[14] and 5.2% for P3HT.[16]

Roll-to-Roll Coated Modules. The production of OPV have until recently been based on spin coating of the active layer in very small area devices with an active area of down to 0.01 cm^2. These devices have been prepared in laboratories worldwide mainly with focus on improving the efficiency of the device. Recently, reports on large area devices (120 cm^2) prepared by R2R coating have been demonstrated. The efficiency of these devices based on P3HT is around 2.1%.[6] We here demonstrate the use of a low band gap polymer in such large area roll-to-roll coated modules. In Figure 5 some pictures from the process of the modules are shown, and the sky blue color of the polymer film is clearly seen.

The photovoltaic responses were measured for all the modules prepared from the batch of the optimized synthesis. Characterization was first done on a R2R solar simulator and then the best modules were cut out and studied by hand. This showed I_{SC} of -0.26 ± 0.02 A cm^{-2}, V_{OC} of 4.38 ± 0.41 V, fill factor of 27 ± 0.5%, and η of 0.31 ± 0.05%. However, the highest efficiency for a single module that was achieved was 0.6% in comparison. Large area R2R coated modules based on PCbzTBT showed very low photovoltaic performances. This is ascribed to the low thermal stability of PCbzTBT[14] resulting in degradation of the polymer during processing in contrast to PDTTDABT, which is stable up to around 300 °C (see Supporting Information for thermogravimetric analysis (TGA) diagram).

Outdoor Testing. The photovoltaic performances of modules (96 cm^2) which were measured outdoor were I_{SC} = 0.13 mA/cm^2, V_{OC} = 10.35 V, FF = 26%, and η = 0.38% (see Supporting Information for IV curves).

Ratio Experiments. In Figure 6 the efficiency is shown as a function of the ratio between donor (PDTTDABT) and acceptor (PCBM) in the active layer as measured in a R2R coating experiment.[17] This demonstrates that the optimum ratio between PDTTDABT and [60]PCBM is 1:2. When the I_{SC}, V_{OC}, and fill factor are plotted as a function of the ratio in the active layer (Figure 7) it can be seen that both I_{SC} and V_{OC} have a maximum at the ratio 1:2, whereas the fill factor is nearly independent of the ratio between polymer and [60]PCBM.

Lifetime Studies of Large Area Modules: Influence of Temperature. In Figure 8, the lifetime studies of selected modules are shown. This shows that PDTTDABT degrades in modules as shown in the photochemical stability studies below. However, the stability is dependent on the temperature of the measurements; i.e., at 80 °C, the lifetime curve

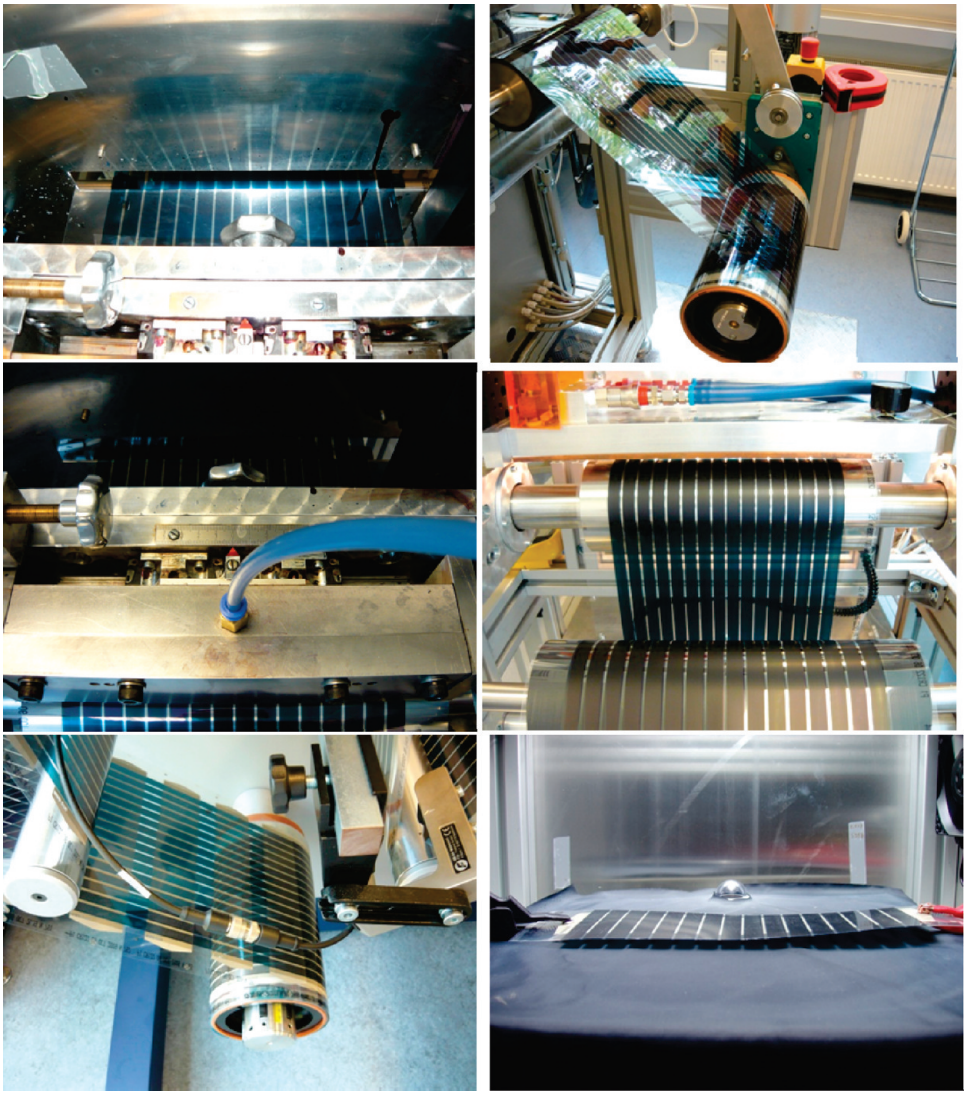

Figure 5. Pictures of roll-to-roll production with PDTTDABT. (Top) Coating of active layer. (Middle) Coating of PEDOT layer. (Bottom) Lamination of the finished modules and test of single module under a solar simulator.

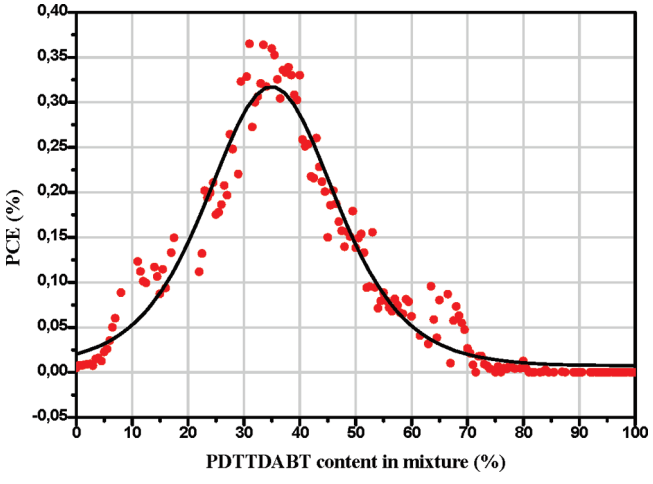

Figure 6. Efficiency as a function of the ratio between PDTTDABT and PCBM in the active layer.

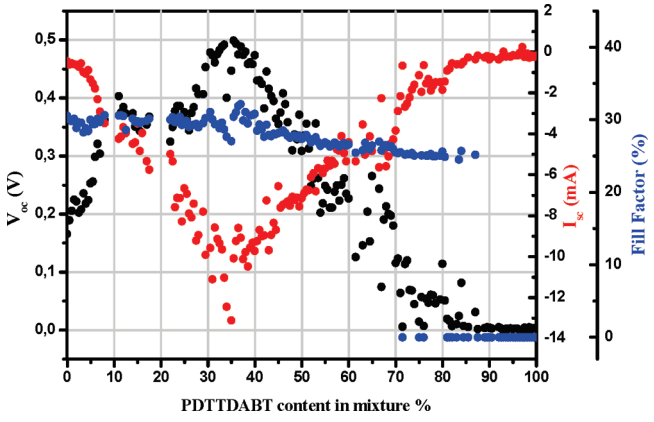

Figure 7. I_{SC}, V_{OC}, and fill factor as a function of ratio between PDTTDABT and PCBM in the active layer.

shows at first an improvement followed by exponential decay, and for temperatures at 50 °C the device performance decreases more slowly.

Photochemical Stability. The results of the photochemical stability studies are shown in Figure 9 and it is seen that photo-oxidation of PDTTDABT resulted in a gradual decay of the optical absorption between 300 and 800 nm. A blue-shift of the absorption maximum—initially located around

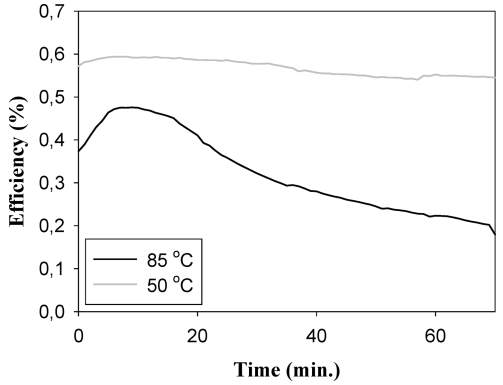

Figure 8. Lifetime studies of modules based on batch 3.

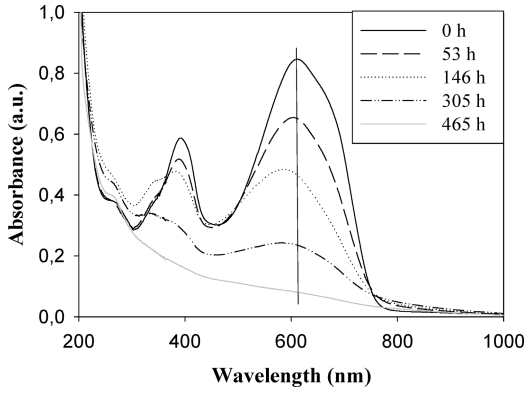

Figure 9. Evolution of PDTTDABT UV−visible absorbance spectrum upon photo-oxidation.

610 nm—was also noticed, indicating a reduction of the π-conjugation length.

PDTTDABT degradation rate was then compared to the one of two reference materials: P3HT and PCbzTBT. P3HT was chosen as it has been the most used polymer in OPVs during the last years. As for PCbzTBT, it is one of the most efficient polymers to date. To fairly compare polymer stability we monitored the total number of absorbed photons versus aging time over the following ranges: 300−700 nm for P3HT and PCbzTBT; 300−800 nm for PDTTDABT. The ASTM G173 standard was used as a reference for the incident photonic flux.[18]

From Figure 10, it is clear that PDTTDABT is the most stable polymer under photo-oxidative conditions. From the lowest to the highest photochemical stability, the ranking is as follows: PCbzTBT, P3HT, PDTTDABT. About 80 h of irradiation resulted in a complete PCbzTBT photobleaching. If one considers P3HT and PDTTDABT, respectively 200 and 500 h were needed to reach an identical stage.

Photo-oxidation also led to strong modifications in the PDTTDABT IR spectrum. Upon irradiation, a disappearance of various functional groups of the polymer was observed (see Supporting Information). Signals characteristic for the dithienothiophene rings (1400 cm^{-1}) and alkoxy groups (1285 cm^{-1}) progressively vanished while new absorption bands developed, for instance in the carbonyl zone (1800−1600 cm^{-1}). The broad complex envelope that progressively developed in this range can be ascribed to products coming from side chains degradation. For longer exposures an intense band was observed around 1110 cm^{-1} and a rather sharp peak was located at 620 cm^{-1}. Interestingly, identical bands have already been observed during P3HT

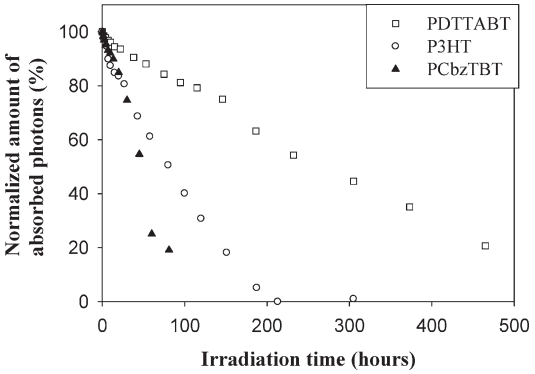

Figure 10. Relative decay of the total number of absorbed photon upon photo-oxidation.

photo-oxidation.[19] They were attributed to the formation of sulfonic esters moieties coming from sulfur oxidation. Here, it seems highly probable that degradation of the dithienothiophene unit leads to the same products. Formation of sulfinic esters implies a ring-opening and thus results in a destruction of the π-conjugated system. This is consistent with the blue-shift observed by UV−visible spectroscopy (Figure 9).

IR monitoring of PCbzTBT aging revealed a rapid decrease in the bands coming from carbazole moieties (1600 cm^{-1}). Signals characteristic for alkyl side chains (3000−2800 cm^{-1}) and C_{sp^3}−N bonds (1330 cm^{-1}) also quickly vanished. Absorption bands pertaining to thiophene and benzothiadiazole groups (e.g., 795 and 1260 cm^{-1} respectively) diminished more slowly. Such results tend to indicate that the relatively low PCbzTBT photochemical stability is due to the presence of the carbazole unit. Instability could likely be linked to the presence of the C_{sp^3}−N bond. Indeed, this bond can be readily cleaved as previously evidenced in the case of polyvinylcarbazole.[20]

Annealing Influence. After thermal treatment of the PDTTDABT and [60]PCBM (1:1) blend for 7 min at 140 °C a very slight absorbance increase is observed while no evolution is recorded by IR. This increase is very probably due to a reorganization of the blend upon the effect of the temperature (annealing). Conversely, an identical thermal treatment of the PCbzTBT and PCBM (1:4) leads to a significant decrease in the absorbance over the whole visible range (see Supporting Information). But, once again, no changes are detected by IR, meaning that this decrease cannot be ascribed to a chemical evolution of the materials. It is also worth noting that no further evolution is observed after a prolonged heating at the same temperature (15 or 25 min).

Conclusions

The use of low band gap polymer, PDTTDABT, in roll-to-roll coated large area devices was successfully demonstrated with photovoltaic efficiencies up to 0.6%. However, it is clear that it is a challenge to design polymers for OPVs prepared by R2R production.

In the design of novel polymers for large area R2R coated OPV modules one has to focus on the alternating of donor and acceptor units (i.e., a low band gap polymer to increase the efficiency) and the side chains (i.e., thermocleavable side chains to increase the stability of the polymer and side chains which ensure solubility and thereby making the R2R production possible). Further, the polymer has to be thermally stable for the production to be possible. We found that in spite of a good thermal, photooxidative, and morphological stability the observed device stability was relatively short. We propose that a low interface stability is responsible for this. In order to have a material for

successful R2R processes, it must in addition to the desired low band gap be photochemically, thermally, and morphologically stable and provide stable interfaces in the devices during operation.

Acknowledgment. This work was supported by the Danish Research Council for Technology and Production (FTP) (Reference No. 274-08-0057).

Supporting Information Available: Figures showing size exclusion chromatography (SEC) spectra, and IV curves, TGA spectra, IR spectra, and absorption spectra before and after annealing and a table of small area OPV device performance data. This material is available free of charge via the Internet at http://pubs.acs.org.

References and Notes

(1) Nielsen, T. D.; Cruickshank, C.; Foged, S.; Thorsen, J.; Krebs, F. C. *Sol. Energy Mater. Sol. Cells* **2010**, *94*, 1553.
(2) (a) Krebs, F. C. *Sol. Energy Mater. Sol. Cells* **2009**, *93*, 394. (b) Helgesen, M.; Søndergaard, R.; Krebs, F: C. *J. Mater. Chem.* **2010**, *20*, 36. (c) Gonzalez-Valls, I.; Lira-Cantu, M. *Energy Environ. Sci.* **2009**, *2*, 19. (d) Ameri, T.; Dennler, G.; Lungenschmied, C.; Brabec, C. J. *Energy Environ. Sci.* **2009**, *2*, 347. (e) Kippelen, B.; Brédas, J. L. *Energy Environ. Sci.* **2009**, *2*, 251.
(3) www.solarmer.com
(4) (a) Krebs, F. C.; Nielsen, T. D.; Fyenbo, J.; Wadstrøm, M.; Pedersen, M. S. *Energy Environ. Sci.* **2010**, *3*, 512. (b) Krebs, F. C.; Fyenbo, J.; Jørgensen, M. *J. Mater. Chem.* **2010**, http://dx.doi.org/10.1039/c0jm01178a (c) Medford, A. J.; Lilliedal, M. R.; Jørgensen, M.; Aarø, D.; Pakalski, H.; Fyenbo, J.; Krebs, F. C. *Optics Express* **2010**, *18*, Issue S3, A286. (d) Krebs, F. C.; Jørgensen, M.; Norrman, K.; Hagemann, O.; Alstrup, J.; Nielsen, T. D.; Fyenbo, J.; Larsen, K.; Kristensen, J. *Sol. Energy Mater. Sol. Cells* **2009**, *93*, 422. (e) Krebs, F. C.; et al. *Sol. Energy Mater. Sol. Cells* **2009**, *93*, 1968.
(5) Jørgensen, M.; Norrman, K.; Krebs, F. C. *Sol. Energy Mater. Sol. Cells* **2008**, *92*, 686.
(6) (a) Krebs, F. C.; Gevorgyan, S. A.; Alstrup, J. *J. Mater. Chem.* **2009**, *19*, 5442. (b) Krebs, F. C.; Tromholt, T.; Jørgensen, M. *Nanoscale* **2010**, *2*, 873. (c) Krebs, F. C. *Sol. Energy Mater. Sol. Cells* **2009**, *93*, 465. (d) Krebs, F. C.; Norrman, K. *ACS Appl. Mater. Interfaces* **2010**, *2*, 877.
(7) Allared, F.; Hellberg, J.; Remonen, T. *Tetrahedron Lett.* **2002**, *43*, 1553.
(8) Helgesen, M.; Gevorgyan, S. A.; Krebs, F. C.; Janssen, R. A. J. *Chem. Mater.* **2009**, *21*, 4669.
(9) Kroon, R.; Lenes, M.; Hummelen, J. C.; Blom, P. W. M.; De Boer, B. *Polym. Rev.* **2008**, *48*, 531.
(10) Chen, J.; Cao, Y. *Acc. Chem. Res.* **2009**, *42*, 1709.
(11) Bundgaard, E.; Krebs, F. C. *Sol. Energy Mater. Sol. Cells* **2007**, *91*, 954.
(12) Winder, C.; Sariciftci, N. S. *J. Mater. Chem.* **2004**, *14*, 1077.
(13) Bundgaard, E.; Krebs, F. C. Chapter in *Energy Efficiency and Renewable Energy through Nanotechnology*; Zang, L., Ed.; Springer: Berlin, 2010, in press.
(14) Park, S. H.; Roy, A.; Beaupré, S.; Cho, S.; Coates, N.; Moon, J. S.; Moses, D.; Leclerc, M.; Lee, K.; Heeger, A. J. *Nat. Photonics* **2009**, *3*, 297.
(15) Scharber, M. C.; Mühlbacher, D.; Koppe, M.; Denk, P.; Waldauf, C.; Heeger, A. J.; Brabec, C. J. *Adv. Mater.* **2006**, *18*, 789.
(16) Ko, C. J.; Lin, Y. K.; Chen, F. C.; Chu, C. W. *Appl. Phys. Lett.* **2007**, *90*, 063509.
(17) Alstrup, J.; Medford, A. J.; Jørgensen, M.; Krebs, F. C. Manuscript in preparation.
(18) Web site for NREL's AM1.5 Standard Dataset: http://rredc.nrel.gov/solar/spectra/am1.5/, accessed on 07/05/2010.
(19) Manceau, M.; Rivaton, A.; Gardette, J.-L.; Guillerez, S.; Lemaître, N. *Polym. Degrad. Stab.* **2009**, *94*, 898.
(20) Rivaton, A.; Mailhot, B.; Robu, S.; Lounaci, M.; Bussière, P. O.; Gardette, J.-L. *Polym. Degrad. Stab.* **2006**, *91*, 565.